

Template-Directed Synthesis of a π -Conjugated Porphyrin Nanoring*

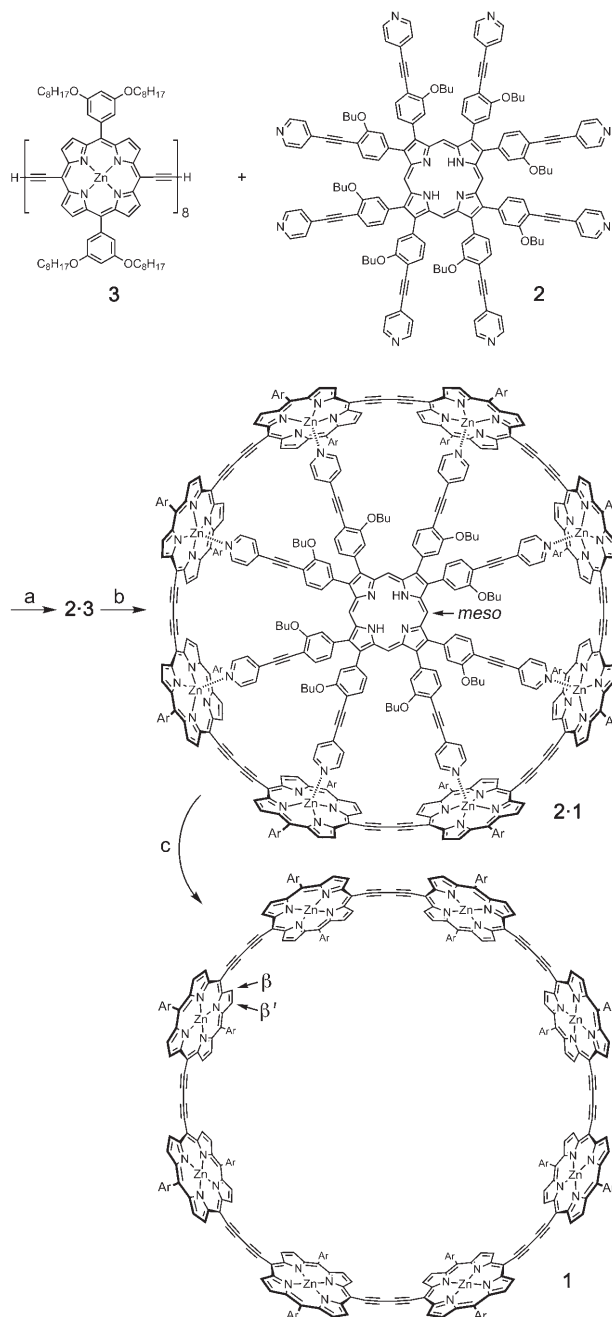
Markus Hoffmann, Craig J. Wilson, Barbara Odell, and Harry L. Anderson*

Large fully π -conjugated macrocycles can be regarded as closed loops of molecular wire. These “wire loops” are expected to exhibit unusual magnetic and optical behavior if the electronic coupling around the ring is sufficiently strong, and recently this idea has led to the synthesis of several large macrocycles.^[1–3] Linear conjugated porphyrin oligomers show strong long-range electronic coupling,^[4–6] and rich nonlinear optical behavior,^[7] thereby providing a motivation for the synthesis of cyclic conjugated porphyrin oligomers. Although many cyclic porphyrin oligomers have been investigated,^[8–14] the vast majority of them lack a complete π -conjugation pathway around the whole macrocycle. The only previously reported conjugated cyclic porphyrin oligomers are the square arrays from the research groups of Sugiura^[13] and Osuka.^[14]

Here we report the template-directed synthesis of a fully conjugated butadiyne-linked cyclic porphyrin octamer **1** with a zinc–zinc distance (between opposite atoms) of 3.4 nm (Scheme 1). Remarkable features of this cyclic octamer include its high symmetry (D_{8h}), its template-directed synthesis by bending a “rigid-rod” linear oligomer, its amazingly high affinity for the template (association constant $K_f = 10^{37} \text{ M}^{-1}$), and its cylindrical belt-shaped structure, which resembles some natural light-harvesting chlorophyll arrays.^[15] Other belt-shaped conjugated systems include fullerenes, carbon nanotubes, anthracene cyclotetramers,^[16] and cyclic *para*-phenylacetylenes (CPPAs).^[17,18] Oda and co-workers have shown that the smooth cylindrical cavities of CPPAs have high affinities for fullerenes and for smaller CPPAs, which leads to the formation of concentric onion-type structures.^[18] The synthesis of cyclic porphyrin octamer **1**, with an internal van der Waals surface diameter of 30 Å, opens the possibility of preparing even larger concentric belts.

Cyclic porphyrin oligomers are particularly amenable to template-directed synthesis by pyridine–zinc ligation,^[8–11] so a key step in our synthesis of cyclic octamer **1** was the design and synthesis of a complementary octadentate ligand **2**. This template has a calculated nitrogen–nitrogen distance (between two opposite pyridyl-N atoms) of 29.6 Å, which is close to the ideal nitrogen–nitrogen distance of 29.0 Å for a

template matching the cavity of cyclic octamer **1** (calculated assuming a Zn–N bond length of 2.2 Å and a displacement of the zinc atom by 0.3 Å from the plane of the porphyrin ring). The design of this template includes eight flexible butyloxy side chains to provide high solubility. The template **2** was



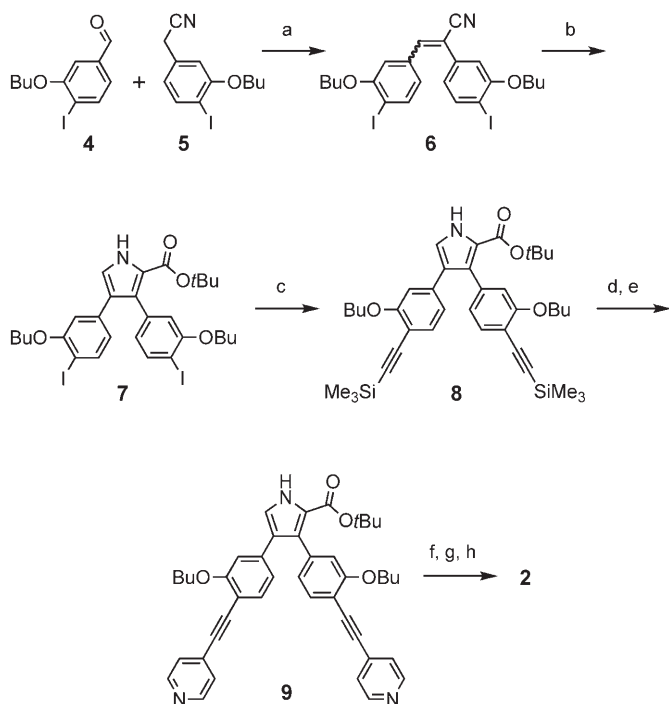
Scheme 1. a) Self-assembly, b) $[\text{PdCl}_2(\text{PPh}_3)_2]$, CuI, $i\text{Pr}_2\text{NH}$, I_2 , air, 60°C , c) pyridine.

[*] M. Hoffmann, Dr. C. J. Wilson, Dr. B. Odell, Prof. H. L. Anderson
Department of Chemistry
Oxford University
Chemistry Research Laboratory
12 Mansfield Road, Oxford, OX1 3TA (UK)
Fax: (+44) 1865-28-5002
E-mail: harry.anderson@chem.ox.ac.uk
Homepage: <http://users.ox.ac.uk/~hlagroup/>

[**] We thank the EPSRC for financial support and the EPSRC Mass Spectrometry Service (Swansea) for mass spectra.

Supporting information for this article is available on the WWW under <http://www.angewandte.org> or from the author.

synthesized by using a Barton–Zard reaction to construct the key pyrrole intermediate **7** from a cyanostilbene **6** (Scheme 2).^[19]



Scheme 2. Synthesis of octadentate template **2**: a) EtONa, EtOH, 77%, b) $\text{CNCH}_2\text{CO}_2\text{tBu}$, KOtBu , THF, 50 °C, 100%, c) $\text{Me}_3\text{SiC}_2\text{H}_5$, $[\text{Pd}_2(\text{dba})_3]$, CuI, PPh₃, Et₃N, 74%, d) Bu_4NF , e) 4-bromopyridine hydrochloride, $[\text{Pd}_2(\text{dba})_3]$, CuI, PPh₃, piperidine, 62%, f) LiAlH_4 , THF, 0 °C, g) TsOH, $\text{CH}_3\text{OCH}_2\text{OCH}_3$, CH_2Cl_2 , h) DDQ, 9% over 3 steps. dba = *trans,trans*-dibenzylideneacetone, TsOH = *p*-toluenesulfonic acid, DDQ = 2,3-dichloro-5,6-dicyano-1,4-benzoquinone.

When the linear porphyrin octamer **3** is titrated with template **2** in chloroform, the changes in the UV/Vis absorption show that a strong 1:1 complex is formed, although the association constant is too strong to measure directly ($K_f > 10^8 \text{ M}^{-1}$; see below). The 1:1 stoichiometry of this complex was confirmed by ^1H NMR titrations. The α - and β -pyridyl protons of the template in the **2·3** complex resonate at $\delta = 2.6$ and 5.4 ppm, respectively, thus proving that all eight coordination sites of the template bind to zinc centers of the linear porphyrin octamer, thereby bending it into a ring and bringing the alkyne terminals into proximity.

Oxidative coupling of the **2·3** complex was achieved under palladium/copper catalysis, using iodine as the oxidant,^[20] to give the cyclic octamer complex **2·1** (55% conversion by gel permeation chromatography (GPC); 14% yield of isolated product). Analytical GPC in THF provided the first clear evidence for the formation of **2·1** (Figure 1). Coupling of linear octamer **3** in the absence of template gives polymeric products which elute faster than **3**, whereas when the reaction is performed in the presence of one equivalent of template **2**, the main product elutes slower than **3** (Figure 1b), as expected for a cyclic oligomer.^[12] Under the conditions of

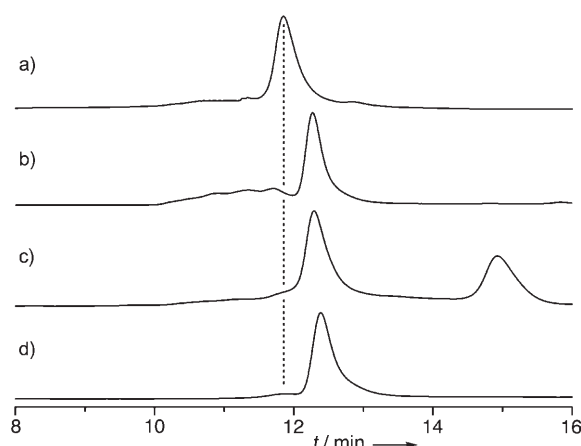


Figure 1. Analytical GPC traces of: a) **3**, b) reaction mixture from the coupling of **2·3**, c) isolated **2·1**, after treatment with pyridine, and d) **1** (absorption signal at 255 nm; THF; flow rate 1 mL min⁻¹; 298 K; 2 × 300 mm, 7.5-mm i.d. PLgel 3- μm Mixed-E columns, Polymer Laboratories Ltd.).

the GPC analysis, the linear octamer complex **2·3** is completely dissociated, whereas the cyclized **2·1** complex remains intact until a large excess of pyridine has been added, when it dissociates to liberate the free template (elution time 15 min; Figure 1c). The hydrodynamic volumes of the free cyclic octamer **1** and its template complex **2·1** are expected to be very similar, so it is not surprising that their GPC traces are identical.

^1H NMR spectroscopic analysis provides excellent evidence for the D_{8h} symmetry of **1**, as illustrated by comparing the resonances corresponding to the β -pyrrole and *meso* protons of **3**, **2·3**, **2·1**, and **1** (Figure 2). The linear octamer **3** should give 16 doublets for the β -pyrrole protons, but most of them overlap, and only the two doublets for the terminal β protons (β_t and β_t') are well resolved (Figure 2a). These

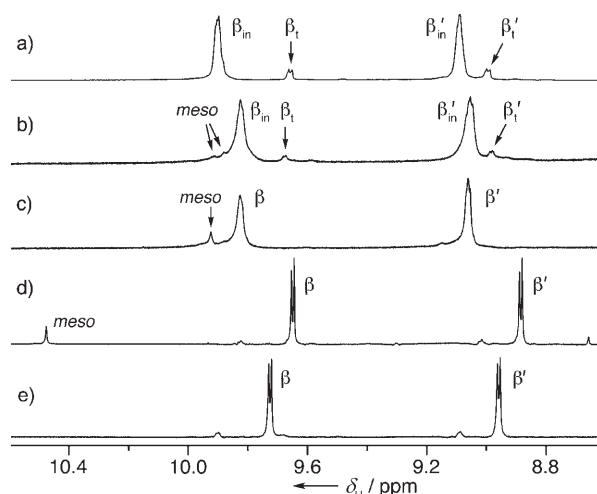


Figure 2. ^1H NMR spectra (CDCl_3 , 328 K, 500 MHz) of: a) **3** with 1 vol% $[\text{D}_5]\text{pyridine}$, b) **2·3**, c) **2·1**, d) **2·1** with 20 vol% $[\text{D}_5]\text{pyridine}$, e) **1** with 1 vol% $[\text{D}_5]\text{pyridine}$. The internal and terminal β -pyrrole protons of **3** are labeled β_{in} and β_t , respectively. See Scheme 1 for the definition of *meso*, β , and β' positions.

resonances shift slightly in the **2**·**3** complex (Figure 2b); the resonance corresponding to the *meso* position of the template is broad and split in this complex because of the reduced symmetry (three *meso* environments). In the **2**·**1** complex this resonance is a sharp singlet and the β protons of the cyclic octamer appear as two poorly resolved pairs of doublets as a result of the D_{4h} symmetry imposed by the template (Figure 2c). On addition of excess [D_5]pyridine (ca. 10^4 equiv) to a solution of **2**·**1**, the resonance corresponding to the template *meso* position shifts downfield by 0.6 ppm as the free template is liberated from the complex, and the resonances of the β protons of the octamer simplify to sharp doublets (β and β' , Figure 2d).

The aryl and alkoxy resonances show that, as expected, the faces of the porphyrin rings are non-equivalent in **2**·**1**, whereas in **1** the external and internal faces of the porphyrins become equivalent on the NMR timescale, probably as a result of rapid rotation of each porphyrin unit around the acetylene axis, with one edge of the porphyrin passing through the large cavity of the cyclic octamer.

The equilibrium constants K_f for formation of **2**·**1** and **2**·**3** are too large to measure directly, but they can be evaluated by measuring how easily pyridine displaces the template (K_b) in the thermodynamic cycle given in Figure 3, which corre-

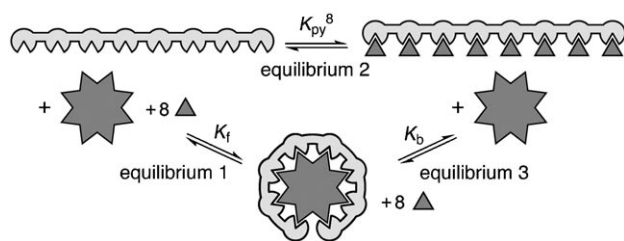


Figure 3. Thermodynamic cycle for binding linear porphyrin octamer **3** (rod) to template **2** (star) and pyridine (triangles). The same cycle also applies to cyclic octamer **1**.

sponds to Equation (1) (K_{py} is the binding constant of pyridine for one zinc center of the porphyrin octamer).^[21]

$$K_f = \frac{K_{py}^8}{K_b} \quad (1)$$

At first sight it may seem surprising that a weak monodentate ligand ($K_{py} = 1.9 \times 10^4 \text{ M}^{-1}$) competes effectively with the octadentate ligand ($K_f \gg 10^8 \text{ M}^{-1}$), but the position of equilibrium 3 depends on the eighth power of the pyridine concentration [Eq. (2)], and during a UV/Vis titration the

$$\frac{[\mathbf{1} \cdot \text{py}]_s}{[\mathbf{2} \cdot \mathbf{1}]} = \frac{K_b [\text{py}]^8}{[\mathbf{2}]} \quad (2)$$

concentration of pyridine can be high ([**py**] up to 10 M) compared to the concentration of the template ($[\mathbf{2}] \approx [\mathbf{1}] \approx 10^{-6} \text{ M}$), so association constants as high as $K_f \approx 10^{46} \text{ M}^{-1}$ are accessible by this type of competition experiment.

The UV/Vis titration results for **2**·**1** and **2**·**3** (Figure 4) show simple isosbestic behavior in both systems, and the binding isotherms fit well to the calculated curve for a two-

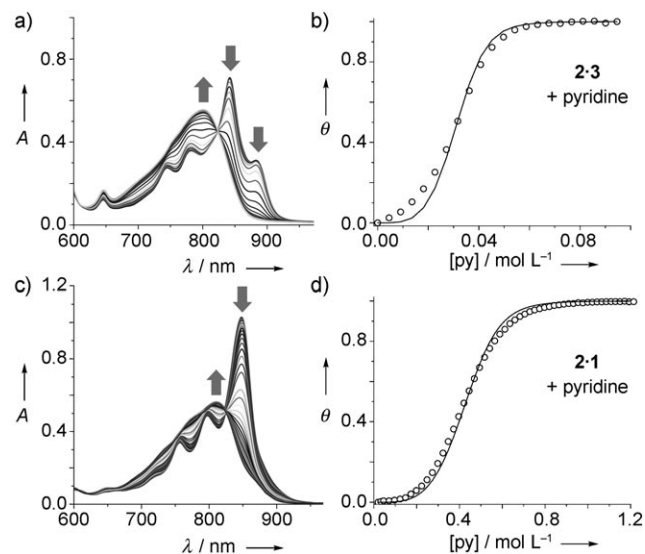


Figure 4. UV/Vis titration spectra and binding curves for **2**·**3** + pyridine (a and b), and **2**·**1** + pyridine (c and d), in CHCl_3 at 298 K (A is absorption; θ is fraction bound; initial concentration of **2**·**3** and **2**·**1**: $3.1 \mu\text{M}$). \circ : data at 858 nm; —: calculated curve.^[22]

state equilibrium^[22] with K_b values of $1.3 \times 10^{-3} \text{ M}^{-7}$ and $1.2 \times 10^6 \text{ M}^{-7}$, respectively, which correspond to K_f values of $1.3 \times 10^{37} \text{ M}^{-1}$ and $1.4 \times 10^{28} \text{ M}^{-1}$ for **1** and **3**, respectively. The host-guest complementarity in these systems can be quantified in terms of effective molarity (EM) according to Equation (3),

$$\text{EM} = \sqrt[7]{\frac{K_f}{(K_0)^8}} \quad (3)$$

where K_0 is the binding constant of one arm of the template for one site on the octamer.

K_0 can be approximated to the binding constant of 4-(phenylethynyl)pyridine to a 5,10-diethynylporphyrin zinc monomer ($K_0 = 1.0 \times 10^4 \text{ M}^{-1}$), which gives EM values of 5.4 M and 0.28 M for **2**·**1** and **2**·**3**, respectively. The difference in the free energies of template binding for **1** ($\Delta G = (-212 \pm 3) \text{ kJ mol}^{-1}$) and **3** ($\Delta G = (-161 \pm 3) \text{ kJ mol}^{-1}$) of 51 kJ mol^{-1} provides an estimate of the energy required to bend the linear octamer into a cyclic conformation. Further experiments will be required to test whether this barrier is mainly enthalpic, thus indicating that **3** behaves as a stiff rod, or entropic, thus indicating that **3** behaves as a flexible chain.

This study demonstrates the power of noncovalent self-assembly for controlling the conformation of porphyrin-based molecular wires, as illustrated previously by torsional control during the formation of double-strand ladder complexes.^[7,21] The synthesis of cyclic octamer **1** also challenges the common perception that molecules such as **3** are “rigid” or “shape-persistent” rods.^[23] It is known that polyynes easily bend into arclike conformations,^[24] and porphyrins are readily dis-

torted.^[25] We suspect that cyclic octamer **1** is not highly strained, and this view is supported by the observation that its absorption spectrum is very similar to that of **3** (Figure 4a,c), whereas the spectrum of **2·1** is sharper and red-shifted relative to that of **2·3**. We are currently exploring the magnetic behavior of the radical cation and radical anion of this cyclic octamer.

Received: November 11, 2006

Published online: February 23, 2007

Keywords: molecular wires · nanostructures · porphyrinoids · self-assembly · template synthesis

- [1] M. Mayor, C. Didschies, *Angew. Chem.* **2003**, *115*, 3284–3287; *Angew. Chem. Int. Ed.* **2003**, *42*, 3176–3179.
- [2] J. Krömer, I. Rios-Carreras, G. Fuhrmann, C. Musch, M. Wunderlin, T. Debaerdemaeker, E. Mena-Osteritz, P. Bäuerle, *Angew. Chem.* **2000**, *112*, 3623–3628; *Angew. Chem. Int. Ed.* **2000**, *39*, 3481–3486.
- [3] S.-H. Jung, W. Pisula, A. Rouhanipour, H. J. Räder, J. Jacob, K. Müllen, *Angew. Chem.* **2006**, *118*, 4801–4806; *Angew. Chem. Int. Ed.* **2006**, *45*, 4685–4690.
- [4] K. Susumu, P. R. Frail, P. J. Angiolillo, M. J. Therien, *J. Am. Chem. Soc.* **2006**, *128*, 8380–8381.
- [5] B. K. Kang, N. Aratani, J. K. Lim, D. Kim, A. Osuka, K.-H. Yoo, *Chem. Phys. Lett.* **2005**, *412*, 303–306.
- [6] P. N. Taylor, J. Huuskonen, G. Rumbles, R. T. Aplin, E. Williams, H. L. Anderson, *Chem. Commun.* **1998**, 909–910.
- [7] a) T. E. O. Screen, J. R. G. Thorne, R. G. Denning, D. G. Bucknall, H. L. Anderson, *J. Am. Chem. Soc.* **2002**, *124*, 9712–9713; b) M. Drobizhev, Y. Stepanenko, A. Rebane, C. J. Wilson, T. E. O. Screen, H. L. Anderson, *J. Am. Chem. Soc.* **2006**, *128*, 12432–12433.
- [8] S. Anderson, H. L. Anderson, J. K. M. Sanders, *Acc. Chem. Res.* **1993**, *26*, 469–475.
- [9] S. Rucareanu, A. Schuwey, A. Gossauer, *J. Am. Chem. Soc.* **2006**, *128*, 3396–3413.
- [10] J. Li, A. Ambroise, S. I. Yang, J. R. Diers, J. Seth, C. R. Wack, D. F. Bocian, D. Holten, J. S. Lindsey, *J. Am. Chem. Soc.* **1999**, *121*, 8927–8940.
- [11] Y. Kuramochi, A. Satake, Y. Kobuke, *J. Am. Chem. Soc.* **2004**, *126*, 8668–8669.
- [12] T. Hori, N. Aratani, A. Takagi, T. Matsumoto, T. Kawai, M.-C. Yoon, Z. S. Yoon, S. Cho, D. Kim, A. Osuka, *Chem. Eur. J.* **2006**, *12*, 1319–1327.
- [13] A. Kato, K. Sugiura, H. Miyasaka, H. Tanaka, T. Kawai, M. Sugimoto, M. Yamashita, *Chem. Lett.* **2004**, *33*, 578–579.
- [14] Y. Nakamura, N. Aratani, H. Shinokubo, A. Takagi, T. Kawai, T. Matsumoto, Z. S. Yoon, D. Y. Kim, T. K. Ahn, D. Kim, A. Muranaka, N. Kobayashi, A. Osuka, *J. Am. Chem. Soc.* **2006**, *128*, 4119–4127.
- [15] G. McDermott, S. M. Prince, A. A. Freer, A. M. Hawthornthwaite-Lawless, M. Z. Papiz, R. J. Cogdell, N. W. Isaacs, *Nature* **1995**, *374*, 517–521.
- [16] a) S. Kammermeier, R. Herges, *Angew. Chem.* **1996**, *108*, 470–472; *Angew. Chem. Int. Ed. Engl.* **1996**, *35*, 417–419; b) R. Herges, M. Deichmann, T. Wakita, Y. Okamoto, *Angew. Chem.* **2003**, *115*, 1202–1204; *Angew. Chem. Int. Ed.* **2003**, *42*, 1170–1172.
- [17] T. Kawase, H. R. Darabi, M. Oda, *Angew. Chem.* **1996**, *108*, 2803–2805; *Angew. Chem. Int. Ed. Engl.* **1996**, *35*, 2664–2666.
- [18] T. Kawase, K. Tanaka, N. Shiono, Y. Seirai, M. Oda, *Angew. Chem.* **2004**, *116*, 1754–1756; *Angew. Chem. Int. Ed.* **2004**, *43*, 1722–1724.
- [19] a) J. L. Bullington, R. R. Wolff, P. F. Jackson, *J. Org. Chem.* **2002**, *67*, 9439–9442; b) D. H. R. Barton, J. Kervagoret, S. Z. Zard, *Tetrahedron* **1990**, *46*, 7587–7598.
- [20] a) J. A. Marsden, J. J. Miller, M. M. Haley, *Angew. Chem.* **2004**, *116*, 1726–1729; *Angew. Chem. Int. Ed.* **2004**, *43*, 1694–1697; b) A. S. Batsanov, J. C. Collings, I. J. S. Fairlamb, J. P. Holland, J. A. K. Howard, Z. Lin, T. B. Marder, A. C. Parsons, R. M. Ward, J. Zhu, *J. Org. Chem.* **2005**, *70*, 703–706.
- [21] P. N. Taylor, H. L. Anderson, *J. Am. Chem. Soc.* **1999**, *121*, 11 538–11 545.
- [22] The binding curves in Figure 4b,d were derived on the basis of Equations (4)–(8), where **M** is either **1** or **3**, and py is pyridine.
$$K_b = ([\mathbf{M}\cdot\text{py}_8][\mathbf{2}]) / ([\mathbf{2}\cdot\mathbf{M}][\text{py}]^8) \quad (4)$$

$$[\mathbf{M}]_0 = [\mathbf{2}\cdot\mathbf{M}] + [\mathbf{M}\cdot\text{py}_8] \quad (5)$$

$$[\mathbf{2}]_0 = [\mathbf{2}\cdot\mathbf{M}] + [\mathbf{2}] \quad (6)$$

$$[\text{py}]_0 = [\text{py}] + 8[\mathbf{M}\cdot\text{py}_8] \quad (7)$$

$$K_b[\mathbf{2}\cdot\mathbf{M}]([\text{py}]_0 - 8[\mathbf{M}]_0 + 8[\mathbf{2}\cdot\mathbf{M}])^8 - ([\mathbf{M}]_0 - [\mathbf{2}\cdot\mathbf{M}])([\mathbf{2}]_0 - [\mathbf{2}\cdot\mathbf{M}]) = 0 \quad (8)$$
- [23] A. Godt, M. Schulte, H. Zimmermann, G. Jeschke, *Angew. Chem.* **2006**, *118*, 7722–7726; *Angew. Chem. Int. Ed.* **2006**, *45*, 7560–7564.
- [24] S. Szafert, J. A. Gladysz, *Chem. Rev.* **2006**, *106*, PR1–PR33.
- [25] J. A. Shelnutt, X.-Z. Song, J.-G. Ma, S.-L. Jia, W. Jentzen, C. J. Medforth, *Chem. Soc. Rev.* **1998**, *27*, 31–41.